DEVELOPMENT, VALIDATION, AND APPLICATION OF A MESOSCALE AMV PRODUCT AT UW-CIMSS

Kristopher Bedka, Christopher Velden, Wayne Feltz, and Ralph Petersen

Cooperative Institute for Meteorological Satellite Studies (CIMSS), University of Wisconsin-Madison
Madison, Wisconsin, U.S.A.

ABSTRACT

Geostationary satellite-derived atmospheric motion vectors (AMVs) have been used over several decades in a wide variety of meteorological applications. The ever-increasing horizontal and vertical resolution of numerical weather prediction models puts a greater demand on satellite-derived wind products to monitor flow accurately at smaller scales and higher temporal resolution. Nowcasting systems for aviation hazards such as turbulence and convection also require accurate upper-air flow information at the mesoscale to detect regions of strong vertical wind shear, ageostrophic flow in jet entrance/exit regions, and locations of developing convection and turbulent outflow.

In an effort to address these needs, work has begun at UW-CIMSS toward the development experimental mesoscale satellite-derived AMV product, which features a significant increase in vector density throughout the troposphere and lower-stratosphere over current NOAA/NESDIS processing methods. Although the more conservative NOAA/NESDIS AMV product exhibits closer statistical agreement to rawinsonde and Wind Profiler observations than the experimental mesoscale AMVs, a comparison of these two products for a selected event shows that the mesoscale product better depicts the circulation center of a mid-latitude cyclone, boundary layer confluence patterns, and a low-level jet present within the warm sector of this system. Thus, while the individual experimental mesoscale AMVs may sacrifice some absolute accuracy, they show promise in providing greater temporal and spatial flow detail which could benefit diagnosis of upper-air flow patterns in near real-time.

1. INTRODUCTION

Operational satellite data processing centers in the U.S., Europe, Asia and Australia routinely produce geostationary AMV datasets several times during each day for the latitude band extending from approximately 60° S to 60° N. Processing of these datasets has been primarily directed toward depiction of larger-scale flow fields with reasonable accuracy for input into global numerical models. However, current and future generation regional mesoscale modeling efforts are beginning to place an increasing demand on accurate satellite-derived products to depict flow variability at smaller scales and higher temporal resolution. Our ability to meet this demand is governed by the spatial, temporal, and spectral resolution of improving satellite instrumentation, as well as assumptions and settings inherent to automated AMV algorithms.

Bedka and Mecikalski (2005) introduced a new AMV processing methodology that extends the current operational NOAA/NESDIS automated algorithm toward depiction of mesoscale flows and their local variability. This experimental mesoscale AMV processing methodology was designed to track cloud and water vapor (WV) features associated with convective clouds at multiple levels within the troposphere, and includes an adjustment of quality-control procedures to allow for significant deviation from a NWP-based background wind analysis. Bedka and Mecikalski demonstrated these so-called “mesoscale” AMVs within an algorithm that computes cumulus cloud top cooling rates, but did not quantitatively assess the relative accuracy of the AMV field.

The objectives of this study are 1) to demonstrate the potential utility of the mesoscale AMV fields for qualitative diagnosis of upper-air flow patterns, 2) to quantify their accuracy relative to co-located rawinsonde and 6-minute NOAA 404 MHz wind profiler observations near the U.S. Department of Energy (DOE) Atmospheric Radiation Measurement (ARM) program Southern Great Plains (SGP) Central Facility at Lamont, Oklahoma (OK), and 3) to demonstrate the utility of 6-minute NOAA Wind Profiler Network observations for satellite-derived AMV validation. The remainder of this paper will provide some perspectives on the use of such a product in U.S. National Weather Service offices across the U.S. Upper Midwest.

2. DATA AND METHODOLOGY

In the development of their experimental mesoscale AMV product (MESO hereafter), Bedka and Meckalski (2005, BM05 hereafter) further adjust the AMV algorithm processing methods described by Rabin et al., in that BM05 acquire MESO from 1 km visible (VIS) and 4 km infrared (IR) window imagery in addition to the water vapor (WV) imagery used by Rabin et al. (2004). The MESO processing scheme represents a variant of the NOAA NESDIS operational AMV algorithm (Nieman et al. 1997, OPER hereafter) processing settings, but greatly increases the vector density that can be derived from the current GOES-12 Imager throughout the troposphere and lower-stratosphere. Major changes include a reduction in both the required AMV agreement with an NWP-based background wind analysis and the size of target boxes that are tracked by the algorithm. Targets in the VIS channel are also tracked up to the 100 hPa level, providing high density flow information from cirrus clouds and convective storm outflow. A complete summary of the primary differences between BM05 MESO and OPER processing is provided in Table 1.

For the statistical validation component of this study, GOES-12 experimental MESO and NOAA/NESDIS OPER AMVs within 25 km of the Lamont, OK 404 MHz NOAA wind profiler site (LMNO2) were collected over a one year period from April 2005-2006, providing a database of 15332 MESO and 1132 OPER VIS, WV, and IR window channel vectors. MESO AMVs are processed every 15-30 mins during the daytime in support of convective storm nowcasting applications which require use of the GOES VIS channel. The MESO processing scheme is by no means limited to daytime operations, but a high percentage of the AMV information is provided through VIS channel cloud tracking. OPER AMVs are processed during both day and night every three hours in support of global NWP model assimilation and other NOAA operations. Both OPER and MESO datasets use a minimum wind speed of 4 ms^{-1} to mitigate depiction of spurious motions that could be caused by errors in satellite data navigation and/or image-to-image registration.

Vaisala RS-92 rawinsonde wind profiles are compared to AMVs and six-minute wind profiler observations to evaluate the relative accuracy of these wind estimates versus an accepted standard for wind measurement. Four rawinsondes are launched per day in normal operations at the SGP Central Facility. When supplemental rawinsondes from intensive observation periods are added to the operational rawinsonde database, quality controlled data from 1628 rawinsondes are included in this study. The measurement accuracy of the Vaisala RS-92 rawinsondes, which uses a Loran-C windfinding system near the ARM SGP site, is estimated to be .5 ms^{-1}. (ARM Balloon Borne Sounding System Handbook, 2005). For reference, the rawinsonde launch site is located 7 km away from the Lamont, OK 404 MHz wind profiler site.

AMV Algorithm Parameter	**MESO Setting**	**OPER Setting**
Target Box Size	5x5 Pixels (~5 km^2 for VIS and ~20 km^2 for IR and WV)	15x15 pixels (~15 km^2 for VIS and ~60 km^2 for IR and WV)
Visible AMV Height Range	1000-100 hPa	1000-600 hPa
Minimum Allowed RFF Analysis Score	0.01	0.50
Minimum Allowed QI Score	0.50	0.60
Gross Speed and Directional Comparison to NWP Forecast	NO	YES
Maximum IR Window Target Temperature	285 K	250 K

TABLE 1: A summary of the primary differences in processing settings between MESO and OPER.

Once proof of profiler measurement consistency and accuracy has been established, a second set of comparisons focuses exclusively on AMV and profiler data matches, which provides a much larger sample size of co-located wind observations. Quality-controlled six-minute resolution data from the Lamont, OK 404 MHz NOAA wind profiler are compared to GOES AMVs to evaluate AMV speed and direction. Since satellite AMVs are height assigned to pressure levels, the profiler sampling levels must be converted from altitude (in meters) to pressure (in hPa) in order to directly compare the two datasets. This conversion is performed using a time-matched initial analysis pressure/height profile from the operational Rapid Update Cycle 20-km resolution model run (RUC-20, Benjamin et al. 2002) for the model grid point closest to the ARM site. As a 3-image sequence of 15-min resolution GOES-12 data is most often used to compute AMVs, at least five of the six possible six-minute wind profiles within this 30-min window are time-averaged together (centered in time on the middle GOES image) in order to remove small scale wind variability and provide a set of wind observations that is reasonable and "fair" to compare with GOES AMVs. Vectors above the 7500 m level are matched only with profiler "high mode" observations, as a much greater number of high mode observations pass quality control checks than those from the low mode within the profiler "overlap-region", extending between 7500 and 9250 m (Petersen and Bedka, 2007).

Comparison 1: Co-located NOAA wind profiler and Rawinsonde				
Datasets Compared	**Number of Matches**	**Horizontal Match Criterion**	**Vertical Match Criterion**	**Temporal Match Criterion**
NOAA Wind Profiler to Rawinsonde	2272	25 km	2 hPa	+/- 3 mins
NOAA Wind Profiler to MESO	2272	25 km	10 hPa	30 min mean profiler data centered on AMV time
Rawinsonde to MESO	2272	25 km	2 hPa	Balloon launch within +/- 30 mins of MESO time
Comparison 2: Co-located NOAA Wind Profiler with MESO and OPER				
NOAA Wind Profiler to MESO	11832	25 km	10 hPa	30 min mean profiler data centered on AMV time
NOAA Wind Profiler to OPER	721	25 km	10 hPa	30 min mean profiler data centered on AMV time

TABLE 3: A summary of dataset match criteria for MESO, OPER, wind profiler, and rawinsonde statistical comparisons

3. APPLICATION OF MESO AMVS TO WEATHER DIAGNOSIS AND FORECASTING

a. June 13, 2005 Event

Before AMV validation statistics are presented, we will first discuss the application of MESO to weather diagnosis and forecasting. This section focuses on an event over the Central U.S occurring on June 13, 2005 with complex flow patterns associated with a mid-latitude cyclone. Figure 1 illustrates the cloud field associated with this weather system as observed by the GOES-12 1 km VIS channel at 1645 UTC. A well-defined cyclonic circulation is centered along the Nebraska-South Dakota border, fair-weather cumulus are to the southeast in the warm sector, and a surface convergence zone (shown in blue) defines the boundary between a very warm, moist air mass present in the southeast U.S. and drier air to the northwest. This boundary served as the focus for severe thunderstorm development later in the day.

Figure 2 shows the AMV fields depicted using both the OPER and MESO methods corresponding the imagery shown in Figure 1. 6239 vectors were identified for this particular image sequence using the MESO method, compared to 1108 conventional OPER winds. Although the primary features of this scene, the cyclonic circulation and southerly flow within the warm sector, are captured by both AMV types, subtle differences exist which have important implications for weather diagnosis and forecasting for this case.

We first focus on mid- to upper-level flow associated with a well-defined cyclonic circulation over the central Great Plains. Analysis of animated multispectral satellite imagery by a human expert positioned the cyclonic circulation over north-central Nebraska at the red X in Fig. 3a and 3c. This is depicted very well by the MESO field (Fig. 3c), but much less so by OPER (Fig. 4d), which portrays a much broader, elongated circulation extending across northern Nebraska and eastern South Dakota. Figure 4b shows that the NOGAPS 6 hour forecast wind field, used as a first guess within the OPER method, also positions the cyclonic circulation further to the east of that shown by MESO. The difference in positions can be attributed in part to the ~1 hour time difference between the NWP and

AMV fields. As this circulation is depicted fairly well by the first guess, the results suggest that the spatial targeting sizes used for OPER IR and WV (15x15 4 km resolution pixels=~60 km^2) were too large to capture this feature. In contrast, the smaller targets (5x5 pixels=~5 km^2 for 1 km VIS and 20 km^2 for 4 km IR and WV) tracked in the upper-troposphere allowed MESO to resolve the mesoscale circulation. The MESO field also captured a region of higher wind speeds (≥ 50 kts) across western Minnesota and the eastern Dakotas (outlined in black), which is represented in the NOGAPS field but completely absent from OPER. These factors further highlight the benefits of detailed feature tracking in detecting subtle regions of enhanced upper-level jet flow.

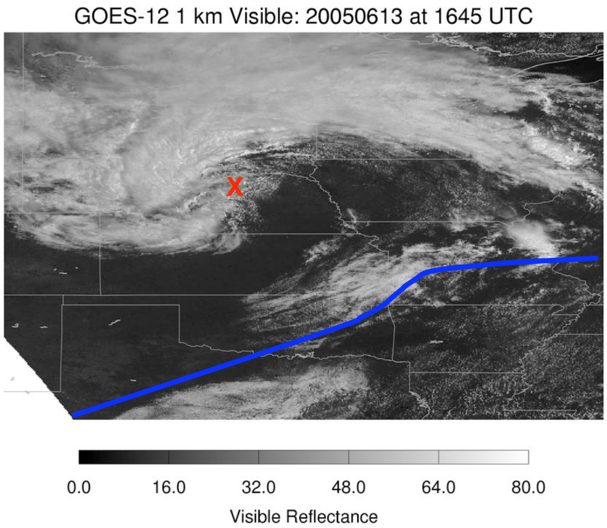

FIGURE 1: GOES-12 1 km Visible imagery on 13 June 2005 at 1645 UTC. The location of a surface convergence line, as identified by a human analyst using surface observations from 1700 UTC, is highlighted in blue separating a warm, humid air mass to the south from drier air north and west of the boundary. The red X illustrates the circulation center of a mid-latitude cyclone.

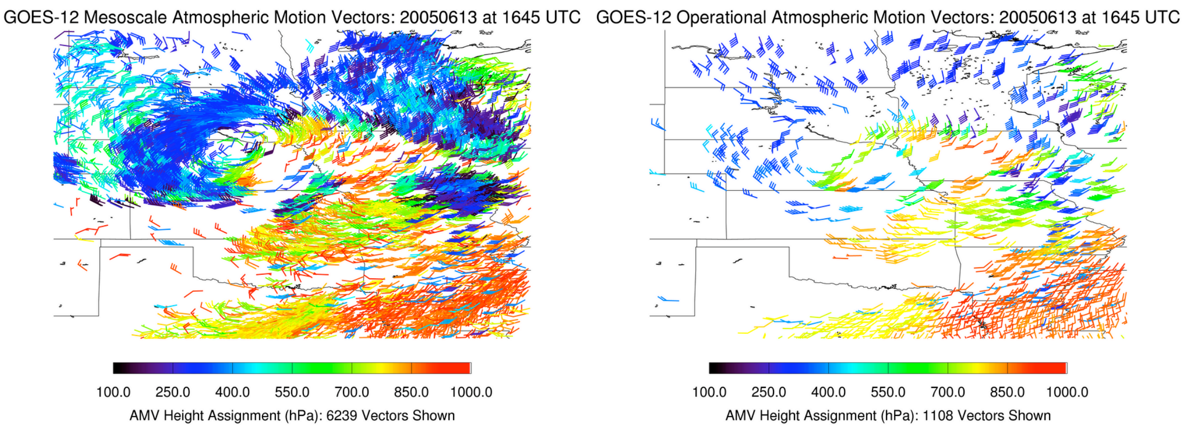

FIGURE 2: (top) MESO over the Central U.S. at 1645 UTC on 13 June 2005. Vectors are colored by AMV height assignment. (bottom) OPER acquired using the same three-image sequence. A full (half) wind barb represents a wind speed of 10 kts (5 kts).

b. MESO AMVs at U.S. National Weather Service Offices

MESO AMV fields have been provided to U.S. National Weather Service (NWS) offices at Milwaukee/Sullivan (MKE) and La Crosse, WI (ARX) from June 2007 to the present time. Figure 4 shows an example of the MESO (white) and OPER (cyan) AMV products with regional NOAA wind profiler (red) atop GOES-12 1 km Visible channel imagery and 300 hPa GFS NWP model streamlines within the NWS AWIPS display framework.

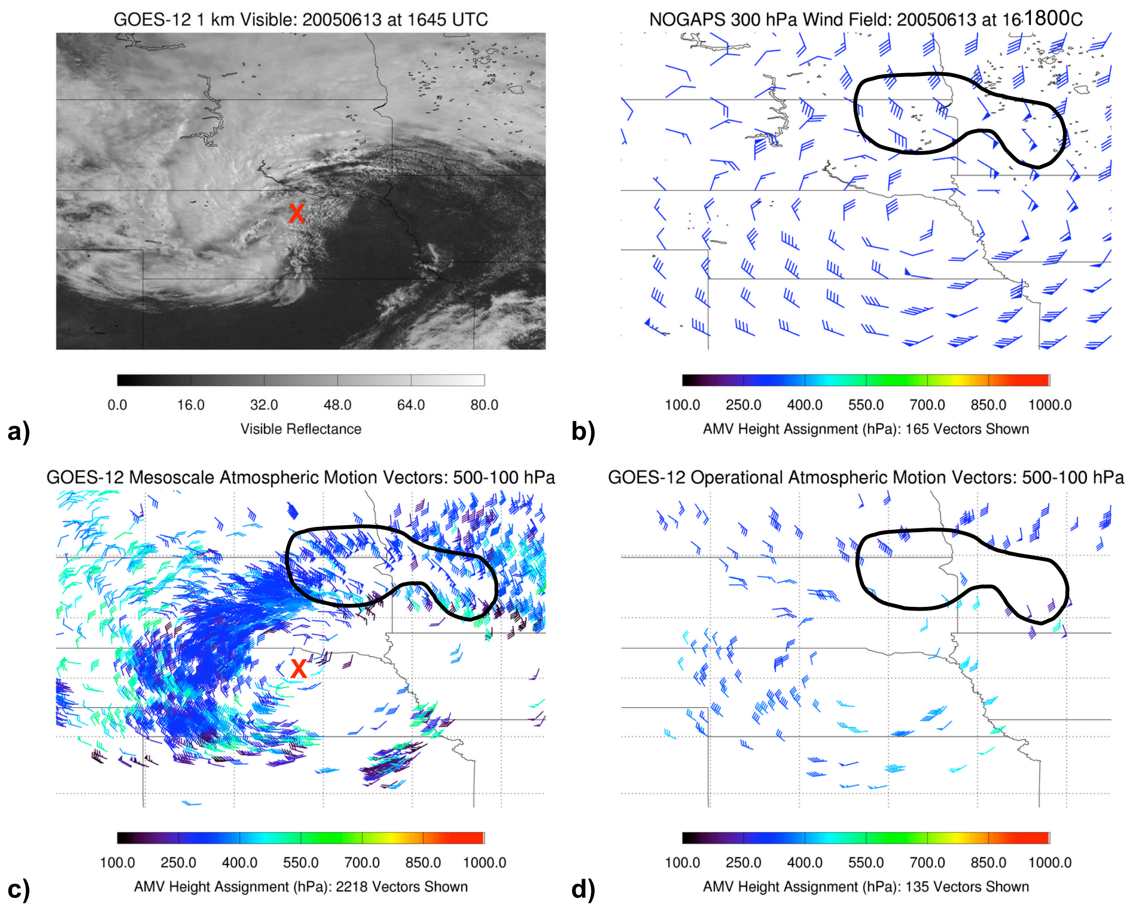

FIGURE 3: (a) GOES-12 1 km Visible channel imagery centered on a closed low pressure center over the U.S. central Great Plains at 1645 UTC. (b) NOGAPS model 6-hour forecast of the 300 hPa wind field valid at 18 UTC. c) All MESO within the 500-100 hPa layer at 1645 UTC. (d) All OPER within the 500-100 hPa layer at 1645 UTC. The red X illustrates the center of circulation of the cloud field as identified by a human analyst. The black line highlights a region of enhanced wind speed captured by MESO and the NOGAPS forecast field that does not appear in the OPER field.

Visualization of the MESO product in conjunction with animated satellite imagery and validation datasets such as NWP and wind profiler within AWIPS can help NWS forecasters: 1) better understand the cloud/WV features being tracked by AMVs, 2) identify value added information provided by AMV relative to profiler, sonde, and NWP, and 3) evaluate errant AMV tracking and height assignment. Feedback from NWS forecasters indicates that they find the MESO AMV product useful for acquiring a detailed synopsis of the wind flow present at a given time. Forecasters have indicated that they do have a preference for a fixed Eulerian wind observing system (i.e. wind profiler) from which they can monitor the flow changes in time, rather than observations that move with the flow (i.e. AMVs) (J.Craven, personal communication). The vast array of upstream data over the U.S. Upper Midwest (sonde, wind profiler, NWP) limits the overall usage of AMVs in their operations, but this may not apply to other regions/offices (i.e. Western U.S. near the Pacific Coast). The forecasters have expressed a desire though for a merged MESO AMV + NWP wind analysis and derived vorticity/divergence fields from the MESO product.

4. QUANTITATIVE AMV VALIDATION

Figure 5 provides a comparison between profiler and sonde wind data where the sonde was within 0-25 km of the profiler site, the same distance criteria that will be used for AMV-profiler comparisons. This comparison shows that VRMS differences between 2 and 3 ms^{-1} are present within the 700-200 hPa pressure layer and there is a significant VRMS increase above and below this layer. The larger low-level differences are likely the result of increased local variability due to mixing processes within and at the top of the boundary layer. The larger differences aloft can be attributed to both increases profiler instrument error and the fact that the decreased vertical resolution of high mode profiler data may not be able to fully capture the strong vertical wind shear which often occurs near the tropopause.

A full description of this comparison and an analysis of spatial and temporal wind variability is provided by Petersen and Bedka (2007). The results of the Petersen and Bedka study and those of Fig. 5 demonstrate that good confidence can be placed in quality controlled 6-minute NOAA Wind Profiler Network data within the 700-200 hPa layer. Though we will compare AMVs to profiler observations within the entire 1000-100 hPa layer in the following section, care must be taken in interpreting the results above 200 hPa.

A comparison between MESO and NOAA wind profiler observations is shown in Figure 6. For the 11832 comparisons shown here, the VRMS (DRMS) is 8.5 ms^{-1} (34°). Bias statistics reveal that the mean MESO speed is .48 ms^{-1} faster than the mean profiler speed, with the mean direction differing by only 1.7°. Scatter point maxima (in greyscale) are found along the diagonal in Fig. 6a-b, and near the origin in Fig. 6c, but a significant number of outliers exist. Points found in the upper-left and lower-right of Fig. 6c are a function of the fact that wind direction varies from 0 to 360°, and do not necessarily represent large differences in direction between MESO and profiler (e.g a direction observation of 359° is very close to a 1° observation). MESO provides “good” wind estimates for 43% of the total vector matches (5087 out of 11832 vectors), if “good” is defined as a vector difference of less than 5 ms^{-1} (not shown). Figure 6d (black bars) shows that MESO matches are well distributed throughout the troposphere, with a slight maximum in the 150-300 hPa pressure layer.

For the 721 OPER and NOAA Wind Profiler comparisons (not shown), the VRMS (DRMS) is 5.6 ms^{-1} (18°). These statistics show that significantly better agreement exists between the coarser resolution OPER and profiler wind observations than those from the larger number of higher resolution MESO comparisons described above. The mean wind speed observed by OPER AMVs is ~3.6 ms^{-1} faster than MESO. This may be related to the fact that ~81% of the data matches are found within the 400-100 hPa layer (see Fig. 6d), which corresponds well with height range of the tropospheric wind speed maximum over the Central U.S. Based upon the above definition, OPER exhibits good agreement with profiler for 65% (469 out of 721 vectors) of the data matches.

375-225 hPa Mesoscale (White) vs. NESDIS Operational (Cyan) Winds

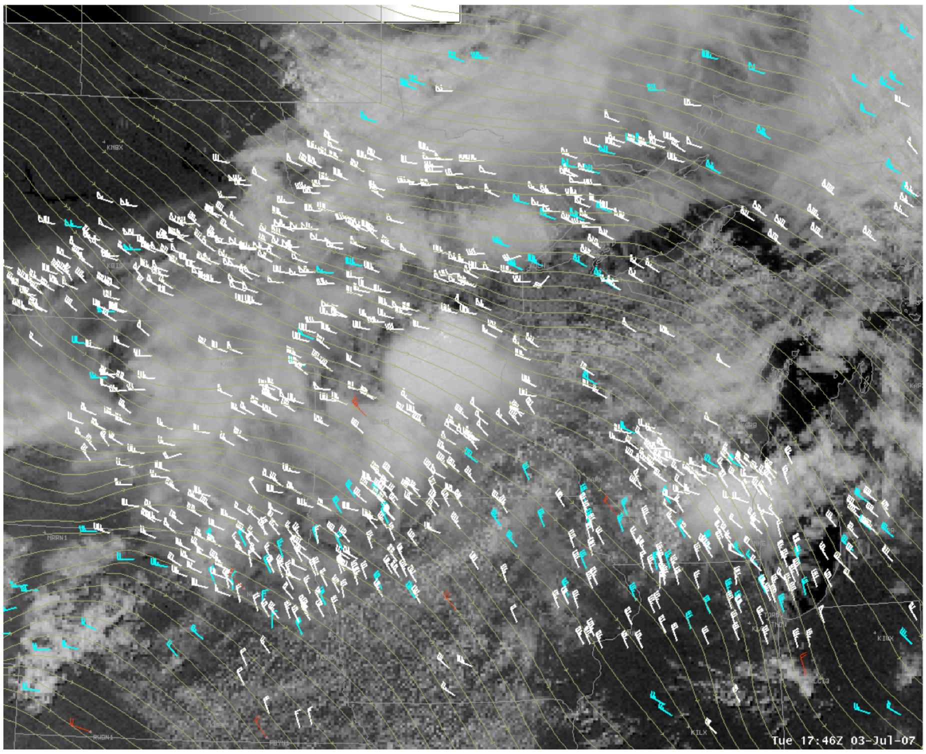

FIGURE 4: An example of the MESO (white) and OPER (cyan) AMV products with regional NOAA wind profiler (red) atop GOES-12 1 km Visible channel imagery and 300 hPa GFS NWP model streamlines (in gold) within the U.S. National Weather Service AWIPS display.

As MESO-profiler differences are significantly larger than those of OPER, we will examine the scene characteristics for significant outliers to better understand scenarios for which MESO and profiler exhibit poor agreement. We consider a significant outlier as a MESO-profiler vector difference greater than 3 standard deviations (SD) from the mean vector difference. The mean (SD) for the 11832 MESO–profiler matches was 6.85 ms^{-1} (5.04 ms^{-1}). We are examining matches with a vector difference greater than ~22 ms^{-1}, which provides 141 vectors for this analysis. GOES-12 animated multispectral imagery is examined for these vectors and three primary scene types were associated with 97% of the outlier AMVs. The three scene types were those featuring cirrus (53% of outliers), multilayered (33%), and cumuliform (both immature and deep convective, 11%) clouds. Thin cirrus and multilayered clouds represent a significant challenge for cloud-top and AMV height assignment algorithms, so the fact these situations represent the vast majority of the outliers is expected.

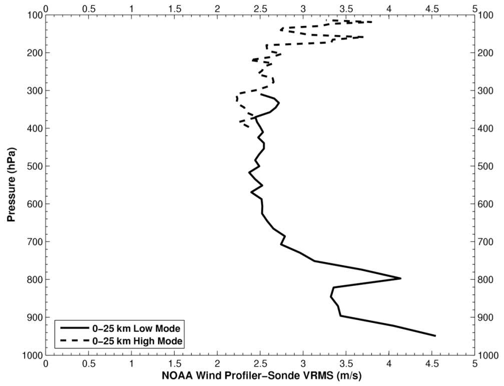

FIGURE 5: The VRMS difference between Lamont, OK 6-minute wind profiler and rawinsonde observations from April 2005-2006 when the rawinsonde was within 25 km of the profiler site.

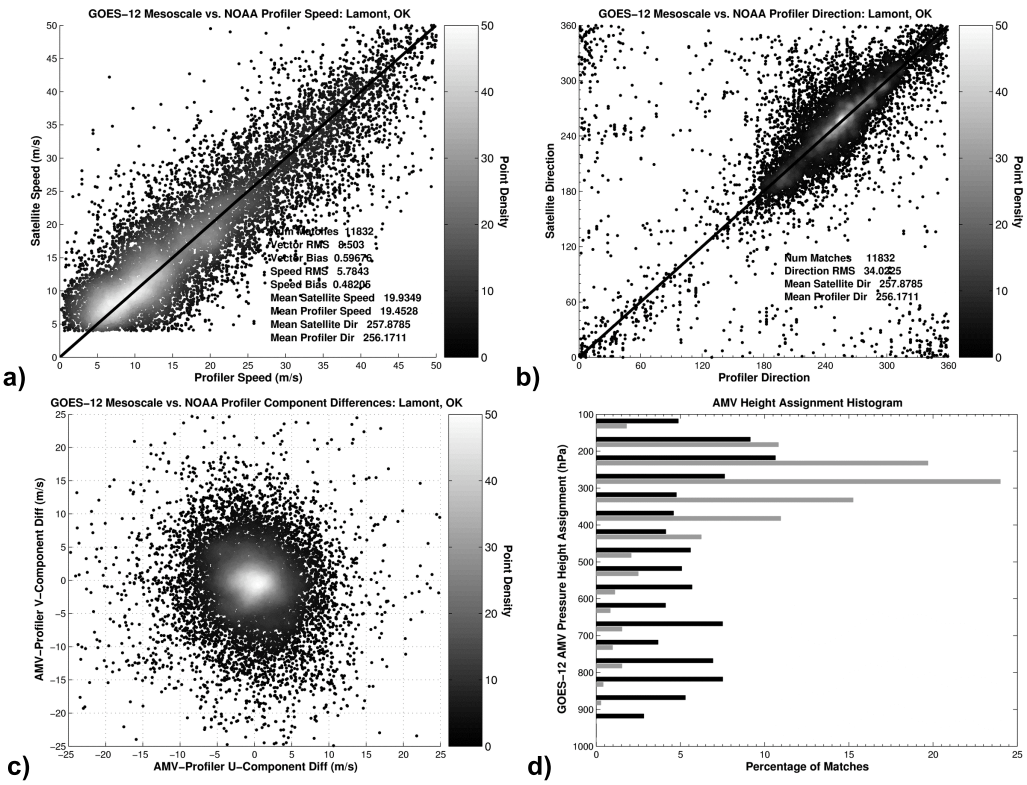

FIGURE 6: A comparison of MESO to NOAA wind profiler (a) speed (in ms^{-1}) and (b) direction for the 1 year study period. (c) MESO versus wind profiler u-component and v-component wind differences. Positive speed biases indicate that the mean AMV wind speed is faster than that observed by wind profiler.

5. CONCLUSIONS

The results of the statistical comparison between AMV and NOAA wind profiler demonstrate that OPER exhibit closer agreement with ground-based observations than individual MESO for all height layers and AMV algorithm quality statistic values. Over a one-year period, the results show that MESO AMVs provide “good” wind estimates (less than 5 ms^{-1} VRMS differences) for 43% of the total vector matches (5087 out of 11832 vectors), compared to 65% (469 out of 721 vectors) for the OPER method. Agreement between AMV and profiler is much closer though for higher QI statistic values and situations when MESO and OPER from near identical scenes agree well (not shown). The MESO method provides a much more even vertical distribution of vectors compared to OPER, where the vectors were concentrated within the 400-100 hPa layer.

Comparisons of co-located 6-minute wind profiler and rawinsonde observations show VRMS differences of ~2.5 ms^{-1} within the 700-200 hPa layer, increasing to over 3.5 ms^{-1} within the stratosphere and near the mean top of the planetary boundary layer and earth surface. Despite the presence of larger VRMS differences at some levels, the stability of the VRMS profile between 700 and 200 hPa in combination with the lack of significant outliers in the profiler-rawinsonde match database suggests that 6-minute ~400 MHz UHF wind profiler data can be used to evaluate and better understand satellite AMV error characteristics.

Although individual MESO estimates may not always be as “accurate” as those depicted by the OPER method, the case event examples shown within this paper and other previous studies illustrate that the vastly increased MESO flow field density can benefit the diagnosis and forecasting of mesoscale weather phenomena in near real-time. Specifically, they provide useful indicators of the presence of low-level confluence, vertical wind shear, convective outflow, and mid- to upper-level divergence and vorticity patterns which are important in forecasting a variety of weather events. One must determine whether greater vector temporal update frequency and spatial flow detail (MESO method) or better relative accuracy (OPER method) will better suit his/her particular application when selecting an AMV processing scheme.

6. REFERENCES

ARM Balloon-Borne Sounding System (BBSS) Handbook, 2005. U.S. Department of Energy, Office of Science.

Bedka, K. M., and J. R. Mecikalski, 2005: Application of satellite-derived atmospheric motion vectors for estimating mesoscale flows. *J. Appl. Meteor.* **44***,* 1761-1772*.*

Benjamin, S.G., J.M. Brown, K.J. Brundage, D. Devenyi, G. Grell, D. Kim, B.E. Schwartz, T.G. Smirnova, T. L. Smith, S. Weygandt, and G.S. Manikin, 2002: RUC20 - The 20-km version of the Rapid Update Cycle. *NOAA/NWS Technical Procedures Bulletin*, NOAA/ERL Forecast Systems Laboratory, Boulder, CO, 2002.

Nieman, S. J., W. P. Menzel, C. M. Hayden, D. Gray, S. T. Wanzong, C. S. Velden, and J. Daniels, 1997: Fully automated cloud-drift winds in NESDIS operations. *Bull. Amer. Meteor. Soc.*, **78**, 1121–1133.

Petersen, R. A., and K. M. Bedka, 2007: Determining the accuracy and representativeness of wind profiler data. 11th Symposium on Integrated Observing and Assimilation Systems for the Atmosphere, Oceans, and Land Surface. 14-18 January 2007, San Antonio, TX.

Rabin, R. M, S. F. Corfidi, J. C. Brunner, C. E. Hane, 2004: Detecting winds aloft from water vapor satellite imagery in the vicinity of storms. *Weather*, **59**, 251-257.